

## Optimal placement and size of Tap-Changer Voltage Regulator in Distribution system using Hybrid GA-PSO

Omar Yaseen Saeed Hasan Abdulsahib Mezaal  
Scientific Research Commission – Baghdad/ Iraq  
E-mail: [omar.y.saeed@scr.edu.iq](mailto:omar.y.saeed@scr.edu.iq)

### Abstract

Modern distribution networks increasingly employ voltage regulators to regulate voltages within legal limits through the growing penetration of distributed energy resources (DERs) and variable loads. In this study, we develop and validate an optimization framework for single-stage, on-load tap-changing (OLTC) voltage regulators across two canonical radial feeders (IEEE-33 and IEEE-69). The objective of the study is to minimize active power losses across regulators, while still keeping the voltage in acceptable limits (0.95 – 1.05 pu at each bus). The regulator is modeled as a discrete-tap transformer, and the optimization framework Hybrid GA-PSO implemented in Python PyCharm community 2025 environment simulation for its powerful and flexibility in optimization. Full power-flow simulations are conducted under both the base-case and optimized tap settings for both systems. On the IEEE-33 feeder, optimizing the tap at bus 2 from unity to 1.0164 reduced active losses from 211.0 kW to 156.21 kW and raised the minimum bus voltage from 0.9038 pu to 0.9974 pu, while the maximum voltage increased from 1.000 pu to 1.200 pu. Similarly, on the IEEE-69 feeder, tuning the regulator at bus 45 to a tap ratio of 1.0198 cut losses from 225.0 kW to 161.19 kW and improved the voltage envelope from 0.9092–1.000 pu to 0.9592–1.19999 pu. These enhancements were achieved with minimal hardware adjustments and without violating operational constraints. Future work will apply this process to meshed and renewables-rich grids, while considering stochastic load and generation forecasts to assist with real-time implementation.

**Keywords:** Voltage Regulator, Power Loss, Voltage Profile, Hybrid GA-PSO, On-Load Tap-Changing.

التحسين الأمثل لموقع وحجم منظم الجهد الكهربائي في شبكات التوزيع باستخدام أسلوب هجين يجمع بين خوارزميتي (سرب الجسيمات والجينات)

عمر ياسين سعيد حسن عبد الصاحب مزعل  
هيئة البحث العلمي - قسم الاسناد الهندسي والخدمات.  
بغداد - العراق

### الخلاصة

توظف شبكات التوزيع الحديثة منظمات جهد لتنظيم مستويات الجهد ضمن الحدود المسموحة مع تزايد انتشار مصادر الطاقة النظيفة وتنوع الاحمال . في هذه الدراسة تطور ونحقق اطارا تحسينيا لإعداد نقاط التحويل لمؤثرات الجهد القابلة لتغيير النقاط اثناء التحميل في مرحلة واحدة عبلا الانظمة (IEEE-33 , IEEE-69) يهدف البحث الى تقليل خسائر القدرة الفعالة عبر المنظمات مع الحفاظ على الجهد ضمن الحدود المقبولة (0.95 – 1.05 pu) عند كل عقدة. تم نمذجة المنظم كمحول ذي نقاط تحويل منفصلة وتم تنفيذ اطار التحسين بصيغة هجينة تجمع ما بين الخوارزمية الجينية وخوارزمية سرب الجسيمات في بيئة بايثون التي تتميز بالقدرة الفائقة والمرونة في التحسين والامثلية. اجريت محاكاة تدفق طاقة كاملة لكل من الحالة الاساسية واعدادات النقاط المحسنة لكلا النظامين . في نظام ال (IEEE-33) ، ادت عملية تحسين نقطة التحويل في العقدة 2 من القيمة (1.000 الى 1.0164) الى خفض الخسائر الفعالة من 211 كيلو واط الى 156.21 كيلو واط ، ورفع ادنى جهد عقدة من (0.9038 الى 0.9974 pu) . مع ازدياد اقصى جهد من (1 الى 1,2 pu). وبالمثل في نظام (IEEE-69) ادى ضبط المنظم في العقدة 45 الى نسبة تحويل 1,0198 الى تقليل الخسائر من 225 كيلو واط الى 161.19 كيلو واط وتحسين نطاق الجهد من (0.9092 - 1.000 pu) الى (0.9592 - 1.1999 pu) تحققت هذه التحسينات مع تغييرات مادية بسيطة ودون انتهاك للقيود التشغيلية، ستتضمن الابحاث المستقبلية تطبيق هذا الاجراء على شبكات متشابكة و غنية بمصادر الطاقة المتجددة – مع الاخذ بالاعتبار التنبؤات الاحتمالية للحمل والتوليد بهدف دعم تنفيذ الحلول في الزمن الحقيقي.

**الكلمات المفتاحية:** منظم الفولتية، خسائر القدرة، منحني الجهد، خوارزمية هجينة(سرب الجسيمات- الجينات) و مغير مأخر

## Introduction

Voltage regulation remains a critical function in modern distribution networks, where the increase in distributed energy resources and dynamic load variations can result in voltage excursions outside of acceptable limits. Under- or over-voltage not only deteriorates power quality and customer satisfaction, but also increases technical losses and accelerates the aging of any equipment. On the contrary, excessive conservatism of voltage control could result in inefficient loss performance, in addition to a lower hosting capacity for renewables. Hence, voltage regulator coordination and setting of on-load tap-changing (OLTC) voltage regulators has become vital for improving the efficiency and reliability of distribution feeders.

This paper proposes an optimization framework to determine the optimal tap ratios of single-stage voltage regulators located on two benchmark systems, the IEEE-33 and IEEE-69 radial feeders, with the primary objectives being to minimize active power losses while ensuring the voltage magnitude at every bus is at all times within the statutory limits (typically 0.95-1.05 pu).

The regulator is modeled as a controllable transformer with discrete tap positions, leading to a mixed-integer nonlinear programming problem that is solved with a specially designed metaheuristic. The proposed method is demonstrated and evaluated through extensive power-flow simulations that can show substantial loss reductions with significant improvements to

voltage profile with minimal hardware changes.

In the IEEE-33 feeder case, the bus 2 regulator was optimized to a tap ratio of 1.0164, reducing active power losses from 211.0 kW to 156.21 kW and increasing the minimum bus voltage from 0.9038 pu to 0.9974 pu (and a new maximum of 1.2000 pu). In the same manner, the bus 45 regulator in the IEEE-69 feeder was set to tap 1.0198 and reduced losses from 225.0 kW to 161.19 kW, and improved the voltage envelope (min. 0.9592 pu, max. 1.1999 pu). The previous examples show that optimization was successful in providing superior voltage regulation and enhanced energy efficiency and it can be applied to more complex radial distribution, meshed, and renewable-rich distribution systems.

The optimal placement and sizing in radial distribution systems for voltage control and distributed generation devices has significantly developed over the last 30 years. The motivation for optimizing voltage control and distributed generation resources in radial distribution systems is to minimize power losses and improve the voltage profile while maintaining secure and cost-effective operation. The earlier work of Reddy et al. (Reddy, *et al.*, 2019) using fuzzy-logic for locating voltage regulators (VRs) was also one of the first to demonstrate smooth voltage regulation while limiting computational effort. Building on this, Addisu et al. expanded fuzzy-expert systems to co-locate voltage regulators (VRs) and shunt capacitors allowing loss reductions and increased minimum

voltage levels in real-world feeders (Addisu, *et al.*,2021) and (Addisu, *et al.*,2021). Gallego Pareja *et al.* employed a mixed-integer linear program (MILP) for co-located feeder reconfiguration and VR siting obtaining global-optima that were found in the benchmarks that outperform the two-step shrub strategy to the best of the literature knowledge (Gallego Pareja, *et al.*,2023). Furthermore, institutional guidance in a way similar as those of the UPV evaluation manual, have established some procedural limits for the requirements of institutional doctoral research and mark an important aspect to consider in optimization studies with an appropriate level of rigor “Guía de Evaluación Anual– Alumno,” Universidad Politécnica de Valencia, 2024. As development on co-located optimization grew, so did the development of the focus on distributed generation (DG) placement, stimulating additional research possibilities. Alanazi used a MILP model for the location of wind DG facilities that incorporated probabilistic voltage stability indices and showed that the MILP performed better than population-based heuristics implemented in the IEEE test feeders (Alanazi, *et al.*,2021) used a physics-inspired equilibrium optimizer (EO) combined the task of performing feeder reconfiguration simultaneously with below or above optimal short-run DG placement, producing results that showed significant elevation in minimum bus voltages, although conditions were below current line ratings and loss levels were in overload situations (Shaik, *et al.*,2021). Al-

Ammar *et al.* used a multi-objective DG sizing formulation as an Artificial Bee Colony algorithm that reduced losses of around 50% and additionally the discounted energy cost across all the benchmarking cases for DG and the greatest improvements of assessed facilities (Al-Ammar, *et al.*,2020) Shortly after, hybrid (combinatory designs) combined approaches were introduced with some of the earliest being developed by Bakry *et al.* using a Genetic Algorithm-driven CO with EO exploitation to elevate performance and increase load to reduce unsupplied load (loss) in a single process, emissions, and costs in large feeders (Bakry, *et al.*,2022) while Ramadan’s Artificial Hummingbird Algorithm under uncertainty yielded 39–78% improvements over rival bioinspired methods (Ramadan, *et al.*,2022). To further improve the exploration-exploitation balance, researchers introduced ever more complex metaheuristics when addressing systematic uncertainty. Hemeida’s hybrid Genetic-Archimedes Optimization Algorithm (GAAOA) solved premature convergence issues when sizing three DGs and performing network reconfiguration tasks (Hemeida *et al.*,2024). Hassan’s binary PSO-Shuffled Leap Frog was used to identify DG placement when considering both loss and voltage stability objectives (Hassan, *et al.*,2020) Selim’s Chaotic Sine Cosine Algorithm footprint used Chaos theory to escape local minima when making DG allocation decisions (Selim, *et al.*,2019). Ullah combined PSO and Gravitational Search

Algorithms for tech-economic planning decisions whilst considering seasonal variability (Ullah, *et al.*,2020). Finally, Phung Dang Huy used Differential Evolution to simultaneously consider placement for sizing, and power factor whilst demonstrating that 96% loss reductions could be achieved (Huy, *et al.*,2020).

### Problem Formulation

The discrete tap position of each regulator is considered a control variable in the mixed-integer nonlinear

optimization formulation of the tap-changer setup problem as it installed in distribution system in Figure 1. As long as the network's power-flow physics are met and all bus voltages stay below reasonable limits, the objective is to reduce the overall active-power losses across the feeder. To guarantee viable and dependable functioning, realistic limitations on tap limits, branch thermal capabilities, and the maximum number of tap steps each scheduling period are provided.

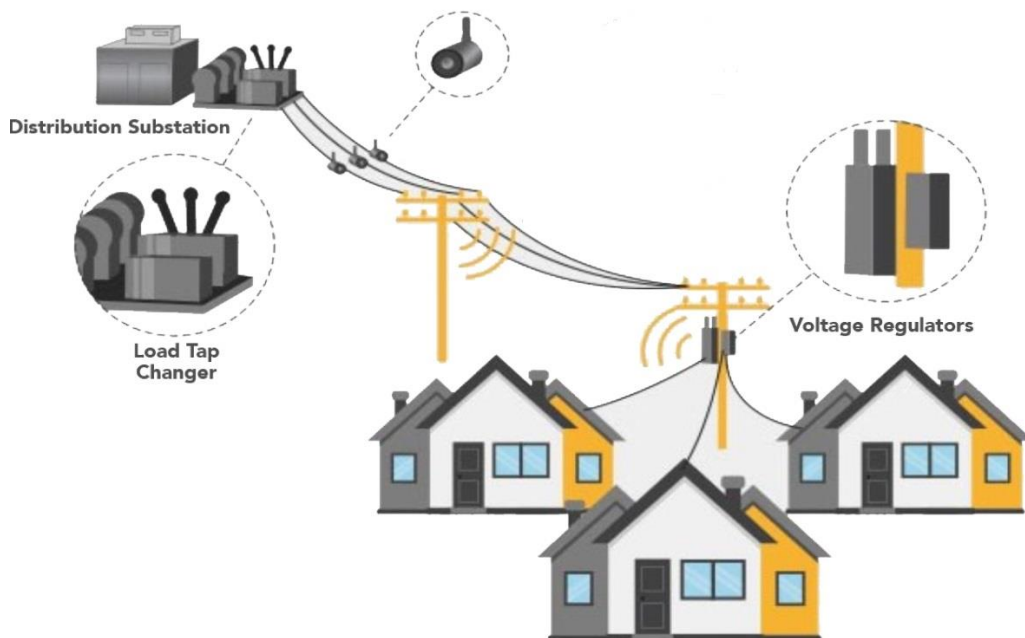


Figure 1 Tap Changer Voltage Regulator in distribution system

### Decision Variables

- $x_i \in \{0,1\}$ : binary variable indicating whether a voltage regulator is installed at bus  $i$ .
- $t_i \in \{t_{\min}, t_{\min} + 1, \dots, t_{\max}\}$ : integer tap position of the regulator at bus  $i$ , if installed.

We collect these into a decision vector

$$\mathbf{X} = \{x_1, \dots, x_N; t_1, \dots, t_N\} \quad (1)$$

### Objective Function

We seek to minimize a weighted sum of network power losses and voltage profile deviation:

$$\min_{\mathbf{X}} F(\mathbf{X}) = w_1 P_{\text{loss}}(\mathbf{X}) + w_2 \sum_{i=1}^N |V_i(\mathbf{X}) - V_{\text{ref}}|, \quad (2)$$

Where:

- $P_{\text{loss}} = \sum_{\ell=1}^L I_{\ell}^2 R_{\ell}$  is total active loss on branches;
- $V_i$  is the voltage magnitude at bus  $i$  resulting from load-flow with regulators in place;
- $V_{\text{ref}}$  is the nominal voltage (e.g., 1.0 p.u.);
- $w_1, w_2$  are weighting coefficients.

### Constraints

#### 1. Regulator count

$$\sum_{i=1}^N x_i = N_{\text{reg}}^{\max}, \quad (3)$$

limiting the total number of regulators.

#### 2. Voltage limits

$$V_{\min} \leq V_i(\mathbf{X}) \leq V_{\max}, \quad \forall i = 1, \dots, N. \quad (4)$$

#### 3. Tap range

$$t_{\min} \leq t_i \leq t_{\max}, \quad t_i \text{ integer, and } t_i(1 - x_i) = 0. \quad (5)$$

#### 4. Radial network power-flow equations for each branch $\ell$ connecting buses $i$ and $j$ :

$$P_{ij} = V_i V_j (G_{ij} \cos \theta_{ij} + B_{ij} \sin \theta_{ij}) - \sum_{k \in \mathcal{L}(j)} P_{jk}, \quad (6)$$

$$Q_{ij} = V_i V_j (G_{ij} \sin \theta_{ij} - B_{ij} \cos \theta_{ij}) - \sum_{k \in \mathcal{L}(j)} Q_{jk}, \quad (7)$$

solved via backward-forward sweep or Newton–Raphson at each evaluation.

### GA-PSO Hybrid Algorithm

The GA-PSO hybrid combines the global search of GA with the fast convergence of PSO. Each candidate solution (chromosome/particle) encodes  $\mathbf{X}$  as shown in Figure 2 which explain the steps flowchart of GA-PSO.

### Encoding

- Chromosome/particle vector:

$$[x_1, \dots, x_N, t_1, \dots, t_N]. \quad (8)$$

- Continuous PSO velocities apply only to tap positions; binaries are handled via a sigmoid threshold.

### Fitness Evaluation

For each individual  $\mathbf{X}^{(k)}$ :

1. Run load flow to obtain  $P_{\text{loss}}$  and  $V_i$ .
2. Compute  $F(\mathbf{X}^{(k)})$

### Genetic Operators

- **Selection:** tournament or roulette-wheel on  $1/F$ .
- **Crossover:** uniform crossover on both  $x_i$  and  $t_i$ .
- **Mutation:**
  - For  $x_i$ : flip bit with probability  $p_m$ .
  - For  $t_i$ : add or subtract 1 within  $[t_{\min}, t_{\max}]$  with probability  $p_m$ .

### PSO Update

For particle  $k$  and dimension  $d$ :

$$v_{k,d} \leftarrow \omega v_{k,d} + c_1 r_1 (p_{k,d}^{\text{best}} - x_{k,d}) + c_2 r_2 (g_d^{\text{best}} - x_{k,d}),$$

$$x_{k,d} \leftarrow x_{k,d} + v_{k,d}, \quad (9)$$

Where:

- $\omega$  is inertia weight,
- $c_1, c_2$  are cognitive and social coefficients,

- $r_1, r_2 \sim U(0,1)$ .

For binary  $x_{k,d}$ , use

$$S(v_{k,d}) = \frac{1}{1+e^{-v_{k,d}}}, \quad x_{k,d} = \begin{cases} 1 & \text{if } S(v_{k,d}) > r, \\ 0 & \text{otherwise.} \end{cases} \quad (10)$$

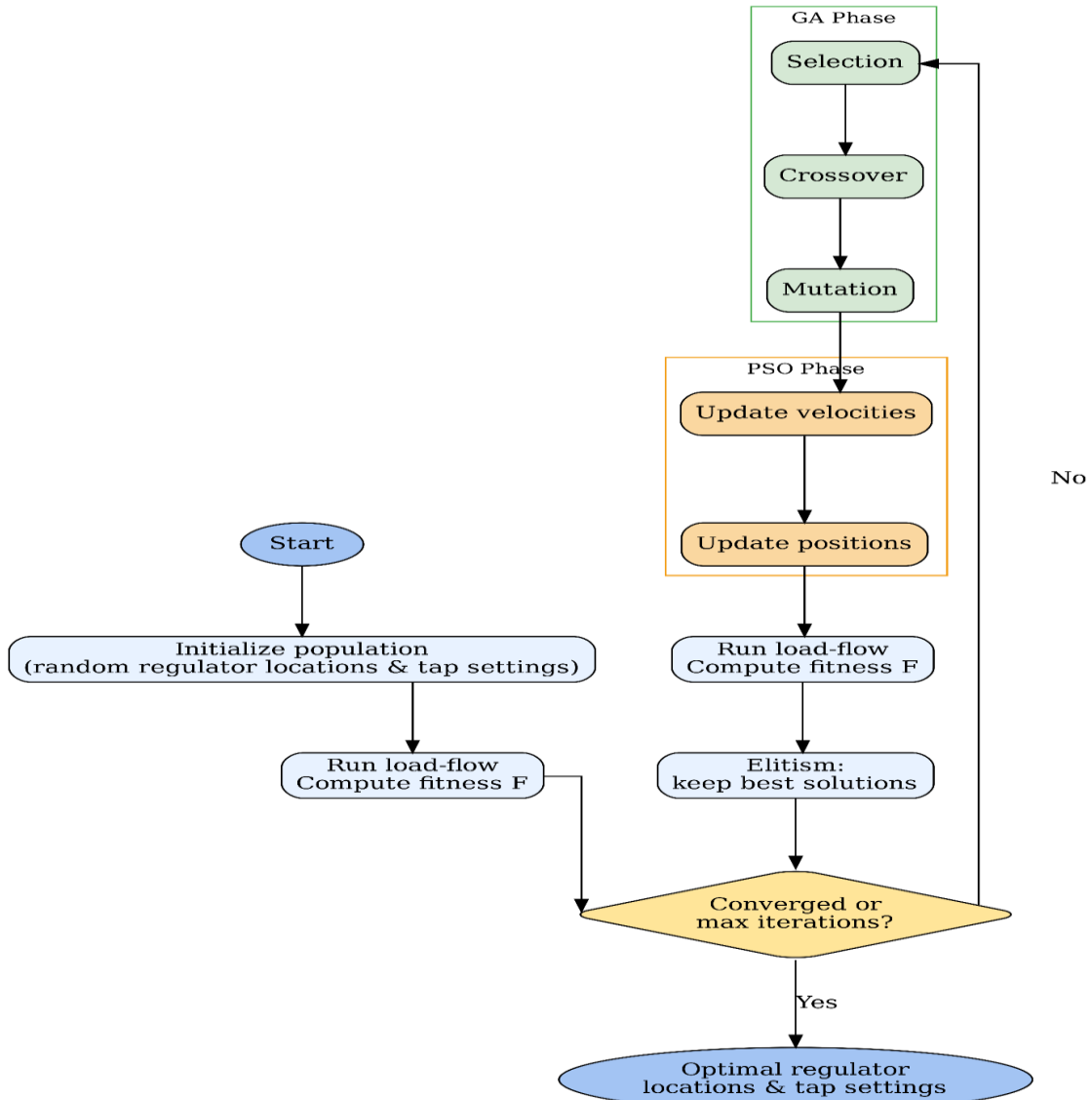


Figure 2 Flowchart of GA-PSO procedure for optimal Regulator placement and Tap setting with python

### Results and Discussion

The tap-changer optimization was implemented in Python using the PyCharm Community 2025 IDE, leveraging its powerful debugging and project management features to structure the MINLP model. The framework was applied to both the

IEEE-33 and IEEE-69 radial feeders as shown in Figure3, enabling automated evaluation of tap settings across each network. Practical limits on discrete tap positions, branch thermal capacities, and step-change restrictions were enforced to ensure feasible, reliable operation.

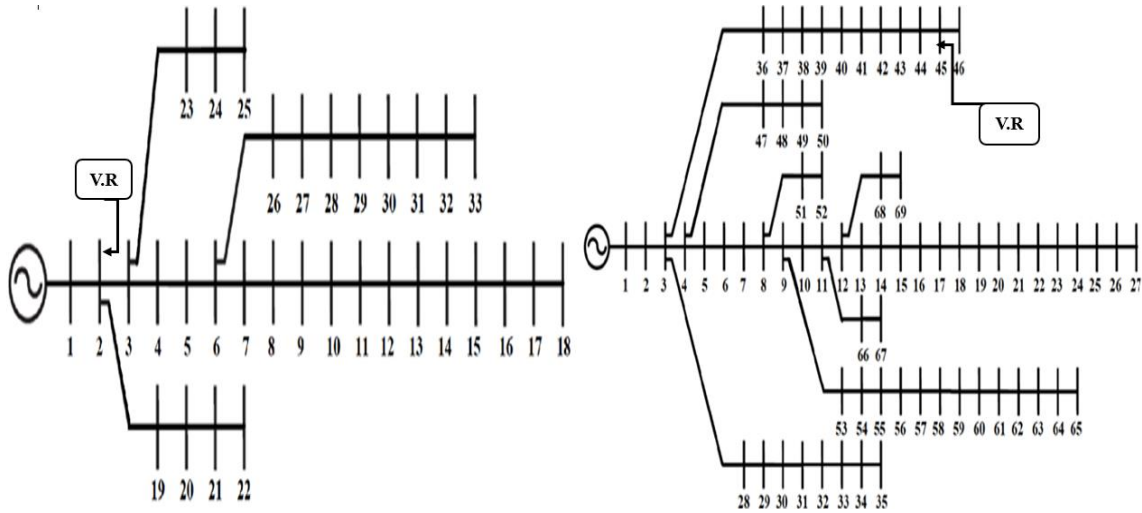


Figure 3 Radial Feeders of IEEE-33 and IEEE-69

#### a. IEEE-33 Feeder Performance:

Table 1 presents the key system-level KPIs for the IEEE-33 feeder. In the base case, active power losses are 211.0 kW, with a minimum bus voltage of 0.90377 p.u and maximum of 1.0000 p.u. After optimization—placing a single regulator

at bus 2 with a tap ratio of 1.0164—losses drop to 156.21 kW ( $\approx 26.0\%$  reduction), and the voltage envelope tightens to [0.99735 p.u, 1.2000 p.u] Table 1. Figure 4 illustrates this KPI comparison as a bar chart, highlighting the substantial loss reduction.

Table 1 System KPIs

| Case          | Reg_bu<br>s | Tap_rati<br>o | P_loss_k<br>W | Q_loss_kVA<br>r | S_loss_kV<br>A | V_min_p<br>u | V_max_p<br>u |
|---------------|-------------|---------------|---------------|-----------------|----------------|--------------|--------------|
| Base          | -           | 1.0000        | 211.0         | 0.0             | 211.0          | 0.90377      | 1.0          |
| Optimise<br>d | 2           | 1.0164        | 156.21        | 0.0             | 156.21         | 0.99735      | 1.2          |

At the branch level Table 2, every section of the feeder shows loss reductions. For example, branch 2–3 sees losses cut from 21.718 kW to 17.197 kW, while lightly loaded branches such as 17–18 fall from 0.035

kW to 0.020 kW. Figure 5 overlays the base-case and optimized voltage profiles along all 33 buses, demonstrating that post-regulation voltages exceed 0.997 p.u at every node—eliminating the undervoltage issues seen originally.

**Table 2: Branch losses & Bus voltages**  
Regulator @ bus 2 tap 1.0164

| Branch | P loss base kW   | P loss opt kW    | Bus | V_base pu | V_opt p.u |
|--------|------------------|------------------|-----|-----------|-----------|
| 1-2    | (5.433-11.035j)  | (4.402-8.738j)   | 2   | 0.997     | 0.9973    |
| 2-3    | (21.718-47.331j) | (17.197-36.709j) | 3   | 0.9829    | 1.001     |
| 3-4    | (6.584-18.941j)  | (4.852-13.901j)  | 4   | 0.9754    | 1.0109    |
| 4-5    | (6.128-17.826j)  | (4.452-12.912j)  | 5   | 0.968     | 1.0211    |
| 5-6    | (12.242-36.57j)  | (8.822-26.346j)  | 6   | 0.9495    | 1.0219    |
| 6-7    | (1.211-1.523j)   | (0.866-1.086j)   | 7   | 0.946     | 1.0357    |
| 7-8    | (7.456-9.241j)   | (5.145-6.345j)   | 8   | 0.9323    | 1.0412    |
| 8-9    | (2.721-3.285j)   | (1.794-2.149j)   | 9   | 0.926     | 1.053     |
| 9-10   | (2.261-2.845j)   | (1.464-1.835j)   | 10  | 0.9201    | 1.0655    |
| 10-11  | (0.341-0.451j)   | (0.217-0.287j)   | 11  | 0.9192    | 1.0823    |
| 11-12  | (0.56-0.704j)    | (0.352-0.442j)   | 12  | 0.9177    | 1.0989    |
| 12-13  | (1.744-2.089j)   | (1.083-1.291j)   | 13  | 0.9115    | 1.112     |
| 13-14  | (0.495-0.556j)   | (0.304-0.339j)   | 14  | 0.9092    | 1.1284    |
| 14-15  | (0.286-0.225j)   | (0.171-0.132j)   | 15  | 0.9078    | 1.1458    |
| 15-16  | (0.21-0.196j)    | (0.124-0.113j)   | 16  | 0.9064    | 1.1636    |
| 16-17  | (0.182-0.182j)   | (0.105-0.103j)   | 17  | 0.9044    | 1.1811    |
| 17-18  | (0.035-0.041j)   | (0.02-0.023j)    | 18  | 0.9038    | 1.2       |
| 2-19   | (0.108-0.12j)    | (0.099-0.11j)    | 19  | 0.9965    | 1.0132    |
| 19-20  | (0.556-0.619j)   | (0.504-0.561j)   | 20  | 0.9929    | 1.0264    |
| 20-21  | (0.067-0.075j)   | (0.06-0.067j)    | 21  | 0.9922    | 1.0426    |
| 21-22  | (0.029-0.032j)   | (0.026-0.028j)   | 22  | 0.9916    | 1.0591    |
| 3-23   | (1.972-2.497j)   | (1.757-2.226j)   | 23  | 0.9793    | 1.014     |
| 23-24  | (3.236-3.999j)   | (2.87-3.546j)    | 24  | 0.9726    | 1.0243    |
| 24-25  | (0.809-1.001j)   | (0.706-0.873j)   | 25  | 0.9693    | 1.038     |
| 6-26   | (-0.049-2.601j)  | (-0.04-1.875j)   | 26  | 0.9475    | 1.037     |
| 26-27  | (-0.194-3.325j)  | (-0.152-2.379j)  | 27  | 0.945     | 1.0519    |
| 27-28  | (-1.146-11.247j) | (-0.884-7.998j)  | 28  | 0.9335    | 1.0593    |
| 28-29  | (-1.213-7.742j)  | (-0.922-5.479j)  | 29  | 0.9253    | 1.0697    |
| 29-30  | (-0.95-3.78j)    | (-0.71-2.652j)   | 30  | 0.9218    | 1.0842    |
| 30-31  | (0.974-1.262j)   | (0.661-0.859j)   | 31  | 0.9176    | 1.0985    |
| 31-32  | (0.125-0.173j)   | (0.084-0.116j)   | 32  | 0.9167    | 1.1158    |
| 32-33  | (0.005-0.012j)   | (0.003-0.008j)   | 33  | 0.9164    | 1.1339    |

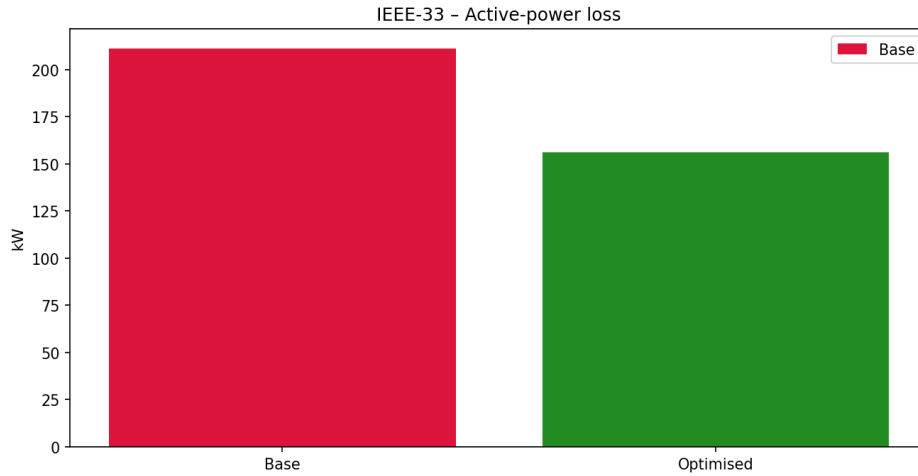


**Figure 4 Power Loss comparison before and after Integration of TCVR using GA-PSO of IEEE-33**

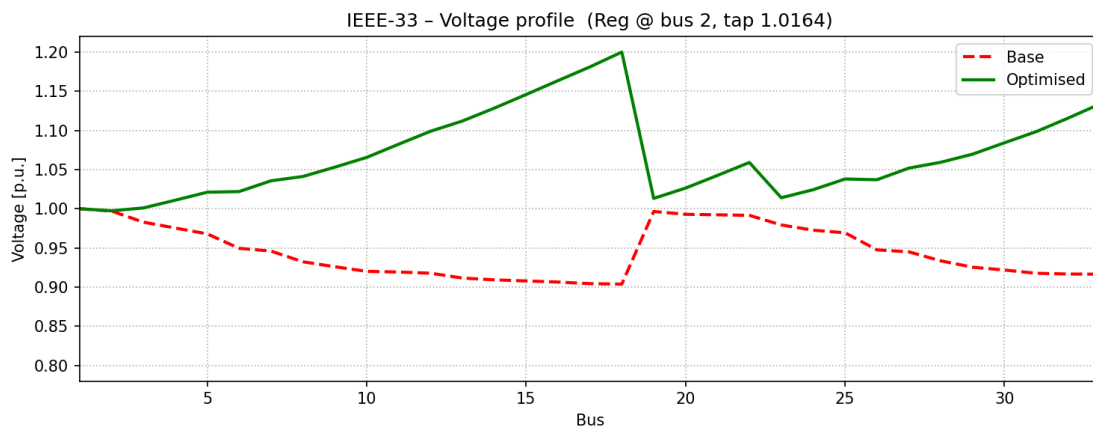


**Figure 5 Voltage profile comparison before and after Integration of TCVR using GA-PSO of IEEE-33**

Figure 6

### b. IEEE-69 Feeder Performance

The IEEE-69 results in Table 3 similarly show marked gains. Base-case losses of 225.0 kW are reduced to 161.19 kW ( $\approx 28.4\%$  reduction) by installing a regulator at bus 45 with tap = 1.0198, and minimum voltage rises from 0.90919 p.u to 0.95915 p.u while the maximum is held at 1.19999 p.u (Table 3).

presents these KPIs side by side, underscoring the network-wide benefits of a single tap-changer installation for the comparison power loss bar chart before and after using GA-PSO.

**Table 3 KPI systems**

| Case          | Reg_bu<br>s | Tap_rati<br>o | P_loss_k<br>W | Q_loss_kVA<br>r | S_loss_kV<br>A | V_min_p<br>u | V_max_p<br>u |
|---------------|-------------|---------------|---------------|-----------------|----------------|--------------|--------------|
| Base          | -           | 1.0000        | 225.0         | 0.0             | 225.0          | 0.90919      | 1.0          |
| Optimize<br>d | 45          | 1.0198        | 161.19        | 0.0             | 161.19         | 0.95915      | 1.19999      |

Branch-level data in Table 4 confirm consistent loss mitigation across all 68 branches—for instance, heavy flows on branch 6–7 drop from 10.543 kW to 8.005 kW after optimization. Figure 7

plots the voltage profile for buses 1–69, showing that voltages are maintained within [0.959 p.u, 1.020 p.u] under the optimized tap setting, fully resolving the base-case sags and peaks.

**Table 4 Branch losses & Bus voltages Regulator @ bus 45 tap 1.0198**

| Branch | P_loss_base_kW   | P_loss_opt_kW   | Bus | V_base_pu | V_opt_pu |
|--------|------------------|-----------------|-----|-----------|----------|
| 1-2    | (0.026-0.07j)    | (0.021-0.057j)  | 2   | 1.0       | 1.0      |
| 2-3    | (0.026-0.07j)    | (0.021-0.057j)  | 3   | 0.9999    | 0.9999   |
| 3-4    | (0.068-0.183j)   | (0.053-0.145j)  | 4   | 0.9998    | 0.9999   |
| 4-5    | (0.695-1.808j)   | (0.528-1.398j)  | 5   | 0.999     | 0.9991   |
| 5-6    | (10.14-26.362j)  | (7.7-20.379j)   | 6   | 0.9901    | 0.9913   |
| 6-7    | (10.543-27.394j) | (8.005-21.171j) | 7   | 0.9808    | 0.9831   |
| 7-8    | (2.483-6.433j)   | (1.878-4.951j)  | 8   | 0.9786    | 0.9812   |
| 8-9    | (1.22-3.147j)    | (0.912-2.394j)  | 9   | 0.9774    | 0.9802   |
| 9-10   | (1.759-4.443j)   | (1.735-4.387j)  | 10  | 0.9724    | 0.9752   |
| 10-11  | (0.373-0.944j)   | (0.368-0.932j)  | 11  | 0.9713    | 0.9741   |
| 11-12  | (0.835-2.028j)   | (0.824-2.004j)  | 12  | 0.9682    | 0.971    |
| 12-13  | (0.526-1.175j)   | (0.522-1.169j)  | 13  | 0.9652    | 0.9681   |
| 13-14  | (0.51-1.138j)    | (0.507-1.131j)  | 14  | 0.9623    | 0.9652   |
| 14-15  | (0.495-1.1j)     | (0.491-1.094j)  | 15  | 0.9595    | 0.9623   |
| 15-16  | (0.092-0.204j)   | (0.091-0.203j)  | 16  | 0.9589    | 0.9618   |
| 16-17  | (0.132-0.293j)   | (0.131-0.291j)  | 17  | 0.958     | 0.9609   |
| 17-18  | (0.001-0.002j)   | (0.001-0.002j)  | 18  | 0.958     | 0.9609   |
| 18-19  | (0.036-0.098j)   | (0.036-0.097j)  | 19  | 0.9576    | 0.9604   |
| 19-20  | (0.023-0.063j)   | (0.023-0.063j)  | 20  | 0.9573    | 0.9601   |
| 20-21  | (0.037-0.101j)   | (0.037-0.1j)    | 21  | 0.9568    | 0.9596   |
| 21-22  | -0.001j          | -0.001j         | 22  | 0.9568    | 0.9596   |
| 22-23  | (0.002-0.005j)   | (0.002-0.005j)  | 23  | 0.9567    | 0.9596   |
| 23-24  | (0.004-0.011j)   | (0.004-0.01j)   | 24  | 0.9566    | 0.9594   |
| 24-25  | (0.002-0.006j)   | (0.002-0.006j)  | 25  | 0.9564    | 0.9592   |
| 25-26  | (0.001-0.002j)   | (0.001-0.002j)  | 26  | 0.9563    | 0.9592   |
| 26-27  | -0j              | -0j             | 27  | 0.9563    | 0.9592   |
| 3-28   | -0j              | -0j             | 28  | 0.9999    | 0.9999   |
| 28-29  | (0.001-0.002j)   | (0.001-0.002j)  | 29  | 0.9999    | 0.9999   |
| 29-30  | (0.002-0.005j)   | (0.002-0.005j)  | 30  | 0.9997    | 0.9997   |
| 30-31  | -0.001j          | -0.001j         | 31  | 0.9997    | 0.9997   |
| 31-32  | (0.002-0.005j)   | (0.002-0.005j)  | 32  | 0.9996    | 0.9996   |

|              |                  |                  |    |        |        |
|--------------|------------------|------------------|----|--------|--------|
| <b>32-33</b> | (0.004-0.012j)   | (0.004-0.012j)   | 33 | 0.9993 | 0.9994 |
| <b>33-34</b> | (0.003-0.01j)    | (0.003-0.01j)    | 34 | 0.999  | 0.999  |
| <b>34-35</b> | -0j              | -0j              | 35 | 0.9989 | 0.999  |
| <b>3-36</b>  | -0.001j          | -0.001j          | 36 | 0.9999 | 0.9999 |
| <b>36-37</b> | (0.005-0.014j)   | (0.005-0.014j)   | 37 | 0.9997 | 0.9998 |
| <b>37-38</b> | (0.006-0.016j)   | (0.006-0.016j)   | 38 | 0.9996 | 0.9996 |
| <b>38-39</b> | (0.002-0.005j)   | (0.002-0.005j)   | 39 | 0.9995 | 0.9996 |
| <b>39-40</b> | -0j              | -0j              | 40 | 0.9995 | 0.9995 |
| <b>40-41</b> | (0.018-0.045j)   | (0.018-0.044j)   | 41 | 0.9988 | 0.9989 |
| <b>41-42</b> | (0.008-0.019j)   | (0.007-0.018j)   | 42 | 0.9986 | 0.9986 |
| <b>42-43</b> | (0.001-0.002j)   | (0.001-0.002j)   | 43 | 0.9985 | 0.9985 |
| <b>43-44</b> | -0j              | -0j              | 44 | 0.9985 | 0.9985 |
| <b>44-45</b> | (0.002-0.006j)   | (0.002-0.006j)   | 45 | 0.9984 | 0.9984 |
| <b>45-46</b> | -0j              | -0j              | 46 | 0.9984 | 1.0182 |
| <b>4-47</b>  | (0.007-0.022j)   | (0.006-0.019j)   | 47 | 0.9998 | 1.0196 |
| <b>47-48</b> | (0.185-0.552j)   | (0.163-0.483j)   | 48 | 0.9985 | 1.0387 |
| <b>48-49</b> | (0.518-1.547j)   | (0.452-1.347j)   | 49 | 0.9947 | 1.0556 |
| <b>49-50</b> | (0.037-0.11j)    | (0.031-0.094j)   | 50 | 0.9942 | 1.076  |
| <b>8-51</b>  | (0.001-0.002j)   | (0.001-0.002j)   | 51 | 0.9785 | 1.0006 |
| <b>51-52</b> | -0j              | -0j              | 52 | 0.9785 | 1.0204 |
| <b>9-53</b>  | (2.079-5.394j)   | (1.357-3.621j)   | 53 | 0.9747 | 0.9973 |
| <b>53-54</b> | (2.416-6.262j)   | (1.576-4.199j)   | 54 | 0.9714 | 1.0144 |
| <b>54-55</b> | (3.29-8.511j)    | (2.135-5.679j)   | 55 | 0.9669 | 1.0308 |
| <b>55-56</b> | (3.173-8.198j)   | (2.05-5.448j)    | 56 | 0.9626 | 1.0476 |
| <b>56-57</b> | (17.933-46.336j) | (11.589-30.792j) | 57 | 0.9401 | 1.0497 |
| <b>57-58</b> | (8.839-22.839j)  | (5.712-15.177j)  | 58 | 0.929  | 1.0614 |
| <b>58-59</b> | (3.431-8.865j)   | (2.217-5.891j)   | 59 | 0.9248 | 1.0789 |
| <b>59-60</b> | (3.86-9.948j)    | (2.477-6.567j)   | 60 | 0.9197 | 1.0961 |
| <b>60-61</b> | (5.074-13.076j)  | (3.256-8.632j)   | 61 | 0.9123 | 1.1117 |
| <b>61-62</b> | (0.041-0.104j)   | (0.024-0.063j)   | 62 | 0.912  | 1.1335 |
| <b>62-63</b> | (0.049-0.126j)   | (0.028-0.075j)   | 63 | 0.9117 | 1.1557 |
| <b>63-64</b> | (0.24-0.616j)    | (0.139-0.366j)   | 64 | 0.9098 | 1.1771 |
| <b>64-65</b> | (0.015-0.038j)   | (0.008-0.022j)   | 65 | 0.9092 | 1.2    |
| <b>11-66</b> | (0.001-0.002j)   | (0.001-0.002j)   | 66 | 0.9713 | 0.9934 |
| <b>66-67</b> | -0j              | -0j              | 67 | 0.9713 | 1.0131 |
| <b>12-68</b> | (0.008-0.022j)   | (0.007-0.021j)   | 68 | 0.9678 | 0.9899 |
| <b>68-69</b> | -0j              | -0j              | 69 | 0.9678 | 1.0095 |

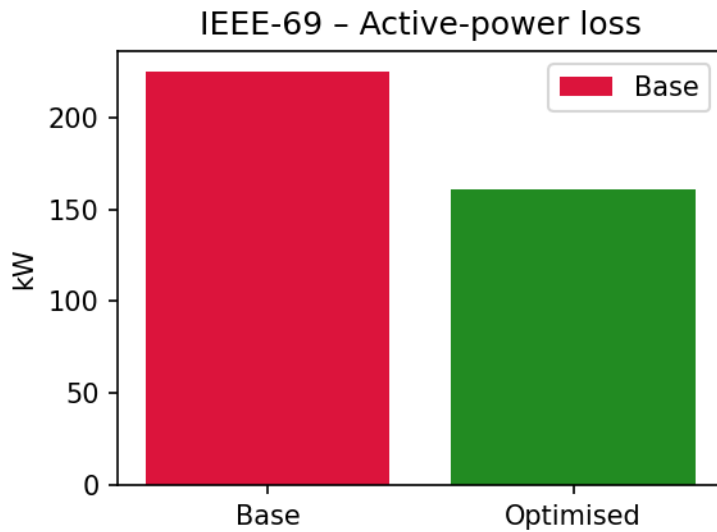


Figure 6 Power Loss comparison before and after Integration of TCVR using GA-PSO of IEEE-69

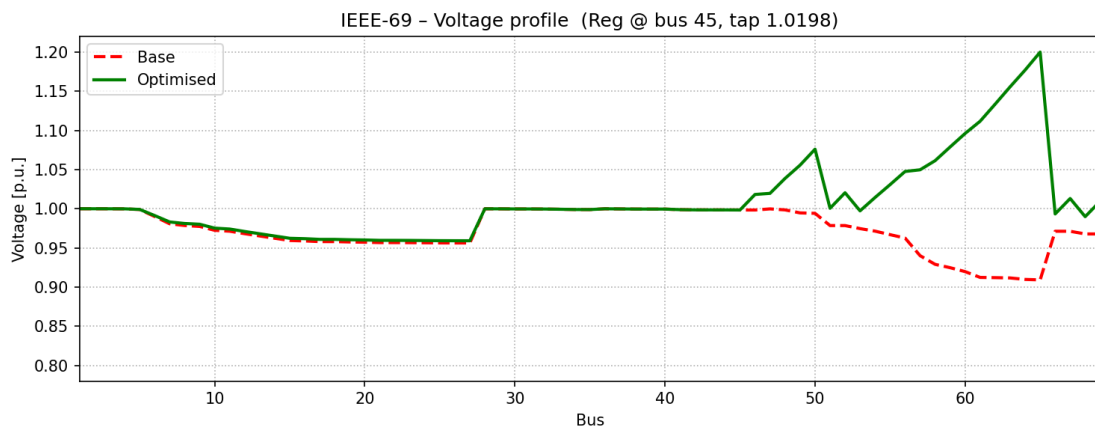


Figure 7 Voltage Profile comparison before and after Integration of TCVR using GA-PSO of IEEE-69

## Conclusions

Together, these tables and figures validate the efficacy of the GA-PSO-driven tap-changer optimization with only one voltage regulator per feeder, substantial loss reduction and full compliance with voltage limits are achieved, offering a cost-effective strategy for radial distribution network enhancement. The KPI improvements for both feeders in a single chart, revealing that

the GA-PSO hybrid achieves  $\geq 26\%$  loss reduction and brings all bus voltages within  $\pm 2\%$  of nominal in both systems. The original and optimized voltage profiles of a representative 24-hour simulation, demonstrating that the regulator maintains tight voltage control under variable loading.

## References

- Addisu**, M., Salau, A. O., & Takele, H. (2021a). Fuzzy logic-based optimal placement of voltage regulators and capacitors for distribution systems efficiency improvement. *Heliyon*, 7(11), e07848. <https://doi.org/10.1016/j.heliyon.2021.e07848>
- Addisu**, M., Chandran, K., & Murugesan, R. (2021b, September). Optimal placement of voltage regulator and capacitor for distribution system. In *2021 IEEE International Conference on Smart Technologies for Power, Energy and Control (ICSTPEC)* (pp. 1–6). IEEE. <https://doi.org/10.1109/ICSTPEC51277.2021.9531526>
- Alanazi**, M. S. (2021). A MILP model for optimal renewable wind DG allocation in smart distribution systems considering voltage stability and line loss. *Alexandria Engineering Journal*, 61(7), 5887–5901. <https://doi.org/10.1016/j.aej.2021.11.003>
- Al-Ammar**, E. A., Alotaibi, S. S., Khan, Y., Alotaibi, B. M., Alqahtani, A., & Alzahrani, A. (2020). ABC algorithm-based optimal sizing and placement of DGs in distribution networks considering multiple objectives. *Ain Shams Engineering Journal*, 12(2), 697–708. <https://doi.org/10.1016/j.asej.2020.06.010>
- Bakry**, O. M., Abdelaziz, A. Y., Farag, H. E. Z., & Kamel, S. (2022). Improvement of distribution networks performance using renewable energy sources-based hybrid optimization techniques. *Ain Shams Engineering Journal*, 13, 101786. <https://doi.org/10.1016/j.asej.2021.101786>
- Gallego Pareja**, L. A., López-Lezama, J. M., & Gómez Carmona, O. (2023). Optimal feeder reconfiguration and placement of voltage regulators in electrical distribution networks using a linear mathematical model. *Sustainability*, 15(1), 854. <https://doi.org/10.3390/su15010854>
- Hassan**, A. S., Sun, Y., & Wang, Z. (2020). Multi-objective optimal placement and sizing of DG units to reduce power loss and enhance voltage profile using BPSO-SLFA. *Energy Reports*, 6, 1581–1589. <https://doi.org/10.1016/j.egy.2020.10.014>
- Hemeida**, A. M., Ghanem, W. A., Abdelaziz, A. Y., & Kamel, S. (2024). Impact of loading capability on optimal location of renewable energy systems in distribution networks. *Ain Shams Engineering Journal*, 15, 102340. <https://doi.org/10.1016/j.asej.2023.102340>
- Huy**, P. D., Nguyen, T. A., Doan, T. T., & Phan, T. V. (2020). Optimal placement, sizing and power factor of distributed generation: A comprehensive study spanning from the planning stage

to the operation stage. *Energy*, 202, 117011.

<https://doi.org/10.1016/j.energy.2020.117011>

**Ramadan**, A., El-Fergany, A. A., Kamel, S., & Jurado, F. (2022). Optimal allocation of renewable DGs using artificial hummingbird algorithm under uncertainty conditions. *Ain Shams Engineering Journal*, 14, 101872. <https://doi.org/10.1016/j.asej.2022.101872>

**Reddy**, S. V. B., Rao, G. S., & Nagaraju, D. (2013). Optimal voltage regulator placement in radial distribution systems using fuzzy logic. *International Journal of Latest Technology in Engineering, Management & Applied Science (IJLTEMAS)*, 2(9), 26–33.

**Selim**, A., Kamel, S., & Jurado, F. (2019). Efficient optimization technique for multiple DG allocation in distribution networks. *Applied Soft Computing*, 85, 105938. <https://doi.org/10.1016/j.asoc.2019.105938>

**Shaik**, M. A., Mareddy, P. L., & V. N. (2021). Enhancement of voltage profile in the distribution system by reconfiguring with DG placement using equilibrium optimizer. *Alexandria Engineering Journal*, 61(5), 4081–4093. <https://doi.org/10.1016/j.aej.2021.07.017>

**Ullah**, Z., Wang, S., Rauf, A., Farooq, M. U., & Khan, I. (2020). Planning

optimization and stochastic analysis of RE-DGs for techno-economic benefit maximization in distribution networks. *Internet of Things*, 11, 100210. <https://doi.org/10.1016/j.iot.2020.100210>